HHS Public Access

Author manuscript

Mater Sci Eng C Mater Biol Appl. Author manuscript; available in PMC 2021 February 01.

Published in final edited form as:

Mater Sci Eng C Mater Biol Appl. 2020 February ; 107: 110290. doi:10.1016/j.msec.2019.110290.

Dual Crosslinking Strategy to Generate Mechanically Viable Cell-laden Printable Constructs using Methacrylated Collagen Bioinks

Nilabh S. Kajave, **Trevor Schmitt**, **Thuy-Uyen Nguyen**, **Vipuil Kishore***

Department of Biomedical and Chemical Engineering and Sciences, Florida Institute of Technology, Melbourne, FL 32901

Abstract

Photopolymerization of methacrylated collagen (CMA) allows for 3D bioprinting of tissue scaffolds with high resolution and print fidelity. However, photochemically crosslinked CMA constructs are mechanically weak and susceptible to expedited enzymatic degradation *in vivo*. The goal of the current study was to develop a dual crosslinking scheme for the generation of mechanically viable cell-laden printable constructs for tissue engineering applications. Dual crosslinking was performed by first photochemical crosslinking of CMA hydrogels using VA-086 photoinitiator and UV exposure followed by chemical crosslinking with two different concentrations of genipin (i.e., 0.5 mM (low dual) or 1 mM (high dual)). The effect of dual crosslinking conditions on gel morphology, compressive modulus, stability and print fidelity was evaluated. Additionally, human MSCs were encapsulated within CMA hydrogels and the effect of dual crosslinking conditions on viability and metabolic activity was assessed. Uncrosslinked, photochemically crosslinked, and genipin crosslinked CMA hydrogels were used as controls. SEM results showed that gel morphology was maintained upon dual crosslinking. Further, dual crosslinking significantly improved the compressive modulus and degradation time of cell-laden and acellular CMA hydrogels. Cell viability results showed that high cell viability (i.e., > 80%) and metabolic activity in low dual crosslinked CMA hydrogels. On the other hand, cell viability and metabolic activity decreased significantly ($p < 0.05$) in high dual crosslinked CMA hydrogels. Quantitative fidelity measurements showed the measured parameters (i.e., line widths, pore size) were comparable between photochemically crosslinked and dual crosslinked constructs, suggesting that print fidelity is maintained upon dual crosslinking. In conclusion, application of low dual crosslinking is a viable strategy to yield mechanically superior, cell compatible and printable CMA hydrogels.

***Corresponding Author:** Department of Biomedical and Chemical Engineering and Sciences, Florida Institute of Technology, 150 W. University Blvd, Melbourne, FL 32901, Tel: 1-(321)-674-8847, Fax: 1-(321)-674-8437, vkishore@fit.edu.

Conflict of Interest: No conflict of interest exist for all authors.

Keywords

methacrylated collagen; dual crosslinking; cell viability; 3D printing

Introduction:

The advent of 3-D bioprinting has allowed for the rapid creation of variable hydrogel-based tissue constructs [1–3]. The physicochemical properties of the constructs can be fine-tuned to emulate the natural characteristics of the extracellular matrix (ECM) using highly customizable hydrogel-based bioinks [4–6]. Bioinks are solutions made of various components, both natural and synthetic, that may be extruded through a needle tip into a prior specified shape and solidified into a stable matrix for use in a variety of different tissue engineering applications [4]. Many studies investigate combinatorial bioinks using collagen type-I, cellulose, gelatin, alginate, and chitosan or synthetic polymers like poly(ethylene glycol) (PEG) [2,4,7]. Often, collagen type-I is used for a cellular scaffold with addition of another natural polymer such as alginate for structural integrity [7,8]. However, addition of alginate as a structural backbone reduces the biomimetic potential of the final scaffold and is associated with limitations such as poor cell adhesion and growth [2]. The use of pure collagen-based bioinks to generate a truly biomimetic scaffold is more meritorious than combinatorial bioinks due to its superior biocompatibility, bioactivity, and the presence of cell-adhesion binding sites [9–11]. Yet, limitations such as low print fidelity, poor mechanical properties, and slower gelation exist [12,13]. The print fidelity of pure collagen-based constructs can be improved by using highly concentrated collagen bioinks, although loss in cellular viability presents a major obstacle with this approach [14]. Therefore, there is a need for an alternative strategy to improve the printability and mechanical properties of pure collagen bioinks while retaining high cellular viability and functionality within the 3D printed constructs.

Chemical crosslinking using agents such as glutaraldehyde and genipin remains a common practice in tissue engineering applications under acellular conditions or with cells seeded atop the scaffolding due to the ability to remove the unreacted crosslinker after tuning the stiffness of the matrix [15,16]. However, for cell-laden 3D bioprinting, cells must interact with the crosslinking solution after printing, wherein the cytotoxicity of the crosslinking solution is a major concern. Recent studies have shown that methacrylation of collagen retains the natural properties of collagen and allows for photochemical crosslinking of collagen-based constructs [17,18]. Methacrylated collagen (CMA), when associated with a photo-initiators such as I-2959 or VA-086, may be exposed to UV light to crosslink the collagen fibers with minimal release of cytotoxic elements and create a cell-laden CMA construct [6,19,20]. While methacrylation and photo-crosslinking of collagen matrices provides structural rigidity suitable for 3D bioprinting, the printed constructs are still mechanically weak and susceptible to rapid enzymatic degradation than that of chemical crosslinking alone [12,18,21].

Application of a dual crosslinking method, that synergizes the advantages of both photochemical crosslinking and chemical crosslinking approaches, can be an effective

strategy for the generation of 3D bioprinted mechanically viable cell-laden collagen constructs. Omobono *et al.* employed photocrosslinking using Rose Bengal photoinitiator together with chemical crosslinking using 1-ethyl-3-(3-dimethylaminopropyl) carbodiimide (EDC) and N-hydroxysuccinimde (NHS) to synthesize mechanically superior cell-laden collagen hydrogels [12]. However, in a separate study, Ibusuki *et al.* reported that the use of Rose Bengal is associated with cytotoxicity [22]. Further, utilizing genipin as a chemical crosslinking solution at low concentrations may be more cytocompatible than EDC and NHS to yield cell-laden collagen hydrogels [23–25].

The primary goal of the current study was to develop a dual crosslinking strategy to improve the mechanical and degradation properties of CMA hydrogels while maintaining high cell viability, metabolic activity, and print fidelity of 3D bioprinted CMA constructs. The dual crosslinking strategy entailed sequential application of photochemical crosslinking followed by chemical crosslinking using genipin. Photochemical crosslinking was performed using VA-086 photoinitiator and UV exposure. Two different genipin concentrations were used − 0.5 mM (low) and 1 mM (high). The effectiveness of this dual crosslinking strategy over either genipin or photochemical crosslinking strategies alone was evaluated using the following assays: (1) Scanning electron microscopy (SEM) to assess the microstructure of the collagen fibers, (2) Uniaxial compression testing to determine compressive modulus, (3) Collagenase degradation test to assess the stability of CMA gels, (4) live-dead cellular viability assay to assess the cytotoxicity, 5) Alamar blue assay to assess cell metabolic activity, and 6) Quantitative geometric measurements to determine print fidelity of 3D bioprinted constructs.

2. Materials and Methods:

2.1 Effect of Genipin Concentration on Cell Viability in 2D Tissue Culture Plate:

Human MSCs (Lonza; PT-2501; hMSC) were expanded in low glucose-DMEM growth medium supplemented with 10% fetal bovine serum (FBS), and 1% penicillin/streptomycin (pen/strep). Cells between passage 5–7 were used for all the experiments.

To determine the optimal genipin concentration to crosslink cell-laden 3D CMA hydrogels, hMSCs were first cultured in 2D tissue culture plates and exposed to different concentrations of genipin (0 mM, 0.25 mM, 0.5 mM, 1mM, 5mM and 10 mM). Briefly, hMSCs were seeded in a 24-well plate at a density of 25,000 cells/cm^2 and cultured for 24 h to allow for cell attachment. Following this, cells were incubated with different concentrations of genipin in 50 mM HEPES buffer for 1 h at 37 °C. Post genipin exposure, cells were washed three times and cultured in alpha-MEM culture medium supplemented with 10% FBS, 1% penicillin/streptomycin, and 10 mM β-glycerophosphate for an additional 24 h. At the end of culture, cells were washed with 1x PBS and stained with calcein AM and ethidium homodimer (Life Technologies) for 15 min at 37 °C and imaged under a fluorescence microscope (Zeiss) to assess the effect of genipin concentration on hMSC viability.

2.2. Synthesis of Dual Crosslinked 3D CMA Hydrogels:

Dual crosslinked CMA hydrogels were prepared by adding a mixture of acid solubilized methacrylated collagen type I solution (3 mg/ml; Advanced BioMatrix, San Diego, CA), 1% w/v VA-086 photoinitiator (Wako, Japan) and 0.1N NaOH (pH = 7.4) into circular rubber washers (7.5 mm diameter, 2.5 mm height) and incubating the mixture at 37 °C for 30 min to induce gelation. After gelation, CMA hydrogels were photochemically crosslinked via UV exposure (365 nm; 17 mW/cm^2) for 1 min. The photochemically crosslinked CMA hydrogels were then subjected to genipin crosslinking by incubating them in 0.5 mM genipin (low dual) or 1 mM genipin (high dual) in 50 mM HEPES buffer (pH 7.4) for 1 h at 37 °C. The upper limit of genipin concentration was 1 mM to maintain viability in cell-laden CMA hydrogels. The effects of dual crosslinking on morphology, mechanics and stability was performed on 3D CMA hydrogels because 1) simple and consistent geometry, and 2) structural similarity with extrusion-based 3D printed solid constructs. Uncrosslinked CMA hydrogels, CMA hydrogels photochemically crosslinked with 1% VA-086 only (1% VA), CMA hydrogels crosslinked with 0.5 mM genipin only (low genipin) and 1 mM genipin only (high genipin) were used as controls.

2.3. Assessment of 3D CMA Hydrogel Morphology using Scanning Electron Microscopy:

The effect of dual crosslinking conditions on fibril morphology and pore-size distribution within CMA hydrogels was evaluated using scanning electron microscopy (SEM). A rigorous sample preparation procedure was employed to minimize the effect of the drying process on fibril morphology within the CMA hydrogels [26,27]. Briefly, CMA hydrogels were serially dehydrated in different concentrations of ethanol solution (20%, 50%, 75%, and 90%) for 15 min each step and treated twice with 100% ethanol for 1 h. Following this, the hydrogels were subjected to critical point drying using Denton DCP-1 dryer, sputter-coated with gold and observed at 8000x magnification under SEM (JEOL JSM-6380LV).

2.4. Effect of Dual Crosslinking on Compressive Properties of 3D CMA Hydrogels:

Uniaxial compression tests were performed to assess the effect of dual crosslinking conditions on the compressive modulus of CMA hydrogels (N = 15/group; DMA Q800, TA Instruments, New Castle, DE). Briefly, CMA hydrogels were mounted between compression clamps in wet condition and an initial preload force of 0.001 N was applied to engage the compression clamp onto the surface of the hydrogel. Following this, the hydrogels were loaded at a rate of 0.01 N/min and the load and the displacement data were collected [18]. Stress was calculated by normalizing the load with the cross-sectional area of the hydrogel and strain was computed by taking the ratio of displacement over the original thickness of the hydrogel. Stress-strain curves were generated and compressive modulus was calculated by determining the slope of the 0–10% strain region [28].

2.5. Effect of Dual Crosslinking on the Stability of 3D CMA Hydrogels:

To determine the stability of dual crosslinked CMA hydrogels (N = 5/group), an *in vitro* collagenase degradation assay was performed [12]. At first, the hydrogels were hydrated in ultrapure water for 30 min. The surface water on the hydrogel was gently blotted off using a kimwipe and the initial weight (W_0) of the hydrogel was determined. Following this, each

CMA hydrogel was incubated in 500 (μl of collagenase solution (5 U/ml in 0.1M Tris-HCl buffer and 5 mM $CaCl_2$; pH 7.4) at 37 °C in microcentrifuge tubes. At periodic intervals, each hydrogel was weighed (W_t) until it was completely degraded. The percent residual mass of the hydrogel at each time point was calculated using the following equation:

$$Resudual\ Mass\ (\%) = \frac{w_t}{w_0} x100$$

2.6. Cell Encapsulation in Dual Crosslinked 3D CMA Hydrogels:

To encapsulate cells within the CMA hydrogels, hMSCs (100,000 cells/ml) were first suspended in neutralized CMA solution with 1% VA-086. Hundred μl of cell suspension was added into each well of a 96-well plate (Corning) and incubated at 37 °C for 30 min to allow for gelation. Following this, the hydrogels were dual crosslinked as described in Section 2.2. These cell-laden 3D CMA hydrogels are structurally similar to extrusion-based 3D bioprinted solid constructs. After crosslinking, the cell-laden hydrogels were washed thrice and cultured in alpha-MEM medium supplemented with 10% FBS and 1% penicillin/streptomycin for 7 days. Cell-laden uncrosslinked CMA, photochemically crosslinked CMA and genipin crosslinked (0.5 mM and 1 mM genipin) CMA hydrogels were used as controls for cell studies.

2.7. Effect of Dual Crosslinking on Cell Viability and Metabolic Activity in Cell-laden 3D CMA Hydrogels:

For cell viability assessment, cell-laden hydrogels (N = 3 hydrogels/group/time point) were transferred to a new culture plate, washed with 1x PBS and stained with Calcein AM and ethidium homodimer for 45 min at 37 °C. After staining, the hydrogels were imaged under a fluorescence microscope (Zeiss) for qualitative assessment for cell viability. In addition, cell viability was quantified via image analyses to determine the percentage of live cells within each hydrogel (N = 5 images/sample/group).

Cell metabolic activity on dual crosslinked CMA hydrogels was assessed using Alamar Blue assay (N = 6 hydrogels/group/time point). At days 1, 4 and 7, cell-laden hydrogels were incubated with 10% Alamar Blue solution (Sigma-Aldrich, MO) at 37 °C for 2 h. Following this, 100 (μl aliquots from each well were transferred to another 96-well plate (Greiner) and fluorescence was measured at an excitation wavelength of 555 nm and an emission wavelength of 595 nm using M2e Spectramax plate reader (Molecular Devices). Relative fluorescence units (RFU) were used as a measure of cell metabolic activity of hMSCs encapsulated within CMA hydrogels.

2.8 3D Bioprinting of Cell-laden Constructs using CMA Bioinks:

A REGEMAT 3D (Granada, Spain) modular-head custom bioprinter was utilized for bioprinting by using the print parameters summarized in Table 1. Cells were encapsulated within a custom bioink solution as described in Section 2.6 and loaded onto the bioprinter. Cell-laden constructs were printed using Freeform Reversible Embedding of Suspended Hydrogels (FRESH) gelatin method to ensure three-dimensional stability [29]. Post printing,

the cell-laden constructs were photochemically crosslinked by exposing them to UV light for 1 min. After UV crosslinking, constructs embedded in FRESH media were incubated at 37 °C and 5% CO_2 for 45 min to melt the gelatin media and recover the printed constructs. Following this, printed constructs were subjected to different genipin crosslinking regimen (i.e., low genipin, low dual) in HEPES buffer for 1 h. Since low genipin crosslinking yielded comparable compressive properties and better cell viability than high genipin crosslinking, high genipin crosslinking was not performed on the printed constructs. The effect of different crosslinking conditions on print fidelity was quantified using ImageJ analyses (National Institute of Health, Bethesda, MD). Briefly, high magnification images of the printed constructs were taken using a DSLR camera (Canon) equipped with a macro lens using a fixed distance. The line measurement function in ImageJ was used to quantify the line width and pore size of the printed constructs. In addition, circularity of the printed discs was measured by taking the ratio of two orthogonal diameters. In addition, the effect of crosslinking conditions on cell viability within printed constructs was assessed using live-dead assay.

2.9 Dual Crosslinking of 3D CMA hydrogels in an Acellular Approach:

Since the CMA hydrogels were devoid of cells in the acellular approach, more vigorous genipin crosslinking conditions can be employed to further improve the mechanical and degradation properties of CMA hydrogels. After photochemical crosslinking, CMA hydrogels were crosslinked with 28 mM (i.e., 0.625% w/v) genipin in 90% ethanol for 24 h at 37 °C [30]. The effect of different crosslinking conditions on compressive and degradation properties was determined as described in Sections 2.4 and 2.5. Uncrosslinked CMA, CMA photochemically crosslinked with 1% VA-086 only (1% VA), and CMA hydrogels crosslinked with 28 mM genipin only were used as controls.

2.10 Statistical Analysis:

Results are expressed as mean ± standard deviation using data combined from at least two independent experiments. Statistical analyses was performed using one-way ANOVA with Tukey post hoc comparisons (JMP Pro 14). Statistical significance was set at $p < 0.05$.

3. Results

3.1 Effect of Genipin Crosslinking Conditions on Cell Viability in 2D Tissue Culture Plate:

To determine the most optimal genipin concentration for crosslinking of 3D CMA hydrogels, human MSCs were exposed to different concentrations of genipin on a 2D culture plate and the effect of genipin concentration on cell viability was determined. Results from the live-dead assay showed that cells remain viable up to 1 mM genipin concentration (Figure 2A–2D). However, increasing the concentration of genipin to 5 mM and 10 mM resulted in significant cell death indicating that genipin at concentrations higher than 1 mM is cytotoxic (Figure 2E, 2F). Based on these results, two different concentrations − 0.5 mM (low) and 1 mM (high) were selected for crosslinking of cell-laden CMA hydrogels in subsequent studies.

3.2 Effect of Dual Crosslinking on Morphology of 3D CMA Hydrogels:

SEM imaging was performed to qualitatively assess the effect of different crosslinking conditions on the morphology of CMA hydrogels. Uncrosslinked CMA hydrogels revealed a fibrous morphology which is a typical characteristic of collagen hydrogels. The fibers observed were thin and loosely packed possibly due to the low concentration of collagen in the hydrogels (3 mg/ml; Figure 3A). Upon crosslinking, no differences in fiber size, fiber orientation, and pore size distribution were observed (Figure 3B–3F). Together, SEM analyses revealed that dual crosslinking does not change the morphology of CMA hydrogels.

3.2. Effect of Dual crosslinking on Compressive Modulus of 3D CMA Hydrogels:

Uniaxial compression tests showed that the compressive modulus of uncrosslinked CMA hydrogels was around 0.2 kPa (Figure 4). Photochemical crosslinking using VA-086 photoinitiator resulted in a significant increase in the compressive modulus of CMA hydrogels. However, crosslinking with genipin only resulted in no change in the compressive modulus of CMA hydrogels. Upon dual crosslinking, the compressive modulus of CMA hydrogels increased around 2-fold compared to uncrosslinked and genipin only crosslinked hydrogels and around 1.3 fold compared to VA-086 photochemical crosslinked hydrogels ($p < 0.05$). Lastly, the compressive modulus of low dual and high dual crosslinked hydrogels was comparable. Together, these results indicate that the dual crosslinking significantly improves the compressive modulus of CMA hydrogels.

3.3 Effect of Dual crosslinking on Stability of 3D CMA hydrogels:

An *in vitro* collagenase degradation assay was performed to assess the effect of different crosslinking conditions on the stability of CMA hydrogels. Results showed that uncrosslinked CMA hydrogels degraded rapidly within 4 hours (Figure 5). The stability of CMA hydrogels improved upon crosslinking as indicated by a significant increase ($p < 0.05$) in the degradation time. Specifically, the degradation time for CMA hydrogels crosslinked with either 1% VA-086 or genipin ranged between 6–8 hours suggesting an almost 2-fold improvement in the stability of the hydrogels ($p < 0.05$). Dual crosslinking further enhanced the stability of the CMA hydrogels. Degradation time for both low dual and high dual crosslinked hydrogels (i.e., 10 hours) was significantly higher ($p < 0.05$) compared to uncrosslinked, 1%VA-086 and genipin only crosslinked CMA hydrogels. Together, these results indicate that dual crosslinking yields more stable CMA hydrogels.

3.5 Effect of Dual Crosslinking on Cell Viability and Metabolic activity in 3D CMA Hydrogels:

Viability of hMSCs encapsulated within crosslinked CMA hydrogels was evaluated using live-dead assay at day 1 and day 7. Results showed that greater than 90% of cells were viable on uncrosslinked CMA hydrogels (Figure 6A). Further, high cell viability was maintained in 1% VA-086, low genipin, and low dual crosslinked CMA hydrogels (Figure 6B, 6C, and 6E). On the other hand, substantial decrease in cell viability was observed in high genipin and high dual crosslinked CMA hydrogels (Figure 6D, 6F). Quantitative cell viability results obtained via image analyses (i.e. the percentage of live vs. dead cells) confirmed the visual observations from the fluorescent images (Figure 6G). Cell viability

was comparable on all hydrogels at day 1. While cell viability was maintained on uncrosslinked, 1% VA-086, low genipin and low dual crosslinked CMA hydrogels from day 1 to day 7, there was a significant decrease in the percentage of live cells in high genipin and high dual crosslinked CMA hydrogels. Specifically, cell viability in high genipin and high dual crosslinked CMA hydrogels decreased from ~80% at day 1 to 54% and 47%, respectively, at day 7 ($p < 0.05$; Figure 6G).

Alamar Blue assay was performed to assess cell metabolic activity within crosslinked CMA hydrogels from day 1 to day 7 (Figure 7A). Results showed that cell metabolic activity in uncrosslinked CMA hydrogels increased significantly from day 1 to day 7 ($p < 0.05$; Figure 6B). Upon crosslinking, cell metabolic activity was observed to increase significantly from day 1 to day 4 and maintain from day 4 to day 7. When comparing between different hydrogels at day 7, cell metabolic activity in uncrosslinked and VA-086 crosslinked CMA hydrogels was comparable. While genipin crosslinking resulted in a significant decrease ($p < 0.05$) in cell metabolic activity compared to uncrosslinked and 1% VA-086 crosslinking conditions, cell metabolic activity was significantly higher ($p < 0.05$) on low genipin and low dual crosslinked hydrogels compared to high genipin and high dual crosslinked hydrogels. Together, these results indicate that low dual crosslinking conditions yield cell-laden CMA hydrogels with high cell viability and cell metabolic activity.

3.6. Effect of Dual Crosslinking on Print Fidelity and Cell Viability in 3D Bioprinted Constructs:

3D bioprinted CMA constructs were qualitatively observed first for deformation compared to the 3D model (Figure 8A) before removal of FRESH media and post removal. All meshes printed with clear mesh structure; however, those that were not photo-crosslinked (Figure 8B and 8D) displayed significant deformation that left fidelity measurements nonviable. Both the 1% VA photo-crosslinked and dual crosslinked meshes survived removal of FRESH medium with pores visible within (Figure 8C and 8E). Quantitative fidelity measurements showed no significant differences in the measured parameters between photochemically crosslinked and dual crosslinked constructs, observing that print fidelity is maintained upon dual crosslinking (Figure 8F–H). Viability staining showed that cells remained viable post-printing in both photo-crosslinked (Figure 8I) and dual crosslinked (Figure 8J) cell-laden constructs.

3.7 Effect of Dual Crosslinking on Mechanical Properties and Stability of 3D CMA Hydrogels in an Acellular Approach:

For the acellular approach, higher concentration of genipin was employed to crosslink the CMA hydrogels. In addition, instead of HEPES buffer which was used for cell-laden CMA hydrogels, genipin crosslinking for the acellular approach was performed in an ethanol-water solution. Results showed the uncrosslinked CMA hydrogels degraded within 6 hours upon collagenase treatment (Figure 9A, 9B). Photochemical crosslinking with VA-086 significantly increased the degradation time to around 10 hours. Upon genipin crosslinking alone and dual crosslinking, there was a sharp increase in degradation time to around 28 hours which was significantly higher ($p < 0.05$) compared to both uncrosslinked and 1% VA-086 photochemically crosslinked CMA hydrogels. The total degradation time for CMA

hydrogels crosslinked with genipin only and dual conditions was comparable. Results from compression tests showed that there was an increase in the compressive modulus of CMA hydrogels upon photochemical crosslinking and genipin only crosslinking, albeit this outcome was not statistically significant (Figure 9C). Compressive modulus of dual crosslinked CMA hydrogels was significantly higher ($p < 0.05$) compared to uncrosslinked and 1% VA-086 crosslinked hydrogels. These results suggest that dual crosslinking improves the mechanical properties and stability of acellular CMA hydrogels.

4. Discussion:

Collagen type-I serves as an excellent bioink base for 3D printed scaffolding due to its ubiquitous presence in natural body tissues. Recent work has shown that the addition of methacrylate groups to the ε-amine groups on the lysine residues of collagen allows for crosslinking of hydrogels via photo-initiated strategies. This process results in methacrylation of approximately 20% of the total amines and has been shown to retain the structural properties of native collagen [31]. However, sole use of photocrosslinking yields hydrogels with limited mechanical rigidity and stability. One approach to further enhance the CMA hydrogel properties is to employ an additional crosslinking step to chemically bond the free amines (i.e., ~80%) that are remaining post methacrylation. Genipin, a primary amine crosslinker derived from gardenia fruits, is known to react with amine groups to form a monomeric adduct which subsequently results in crosslinking of the collagen protein [30,32,33]. The current study is the first attempt to employ a dual crosslinking scheme that leverages the advantages of both photochemical crosslinking and genipin crosslinking methods to enhance the mechanical and degradation properties of 3D printed pure collagen constructs while maintaining high cell viability and print fidelity. These cell-laden collagen constructs can be printed to resemble the compositional and structural aspects of native tissue and hence have immense biomimetic potential for use in a variety of different tissue engineering and regenerative medicine applications.

The impact of genipin on cell viability must be addressed, though prior work has shown that genipin is less cytotoxic than other chemical crosslinking solutions [30,34]. Lower concentrations of genipin will yield higher cell viability, yet scaffold mechanics suffer for it, requiring a delicate balance to maintain both cell viability and mechanical properties of the scaffold [16,25]. While an acellular approach allows for the use of far greater genipin concentrations, and thus yield greater mechanical stiffness, this becomes nonviable when cells have extended contact with the chemical crosslinker. Therefore, to first determine the optimal genipin concentration for viable cell encapsulation in CMA hydrogels, hMSCs were directly exposed to different genipin concentrations in a 2D culture plate. Results showed an overwhelming cytotoxic effect at genipin concentrations greater than 1 mM (Figure 2). Further, 1 mM was shown to reduce cellular viability to a noticeable degree (Figure 2D). For this reason, 0.5 mM (low) and 1 mM (high) concentrations of genipin were selected for genipin crosslinking of cell-laden CMA hydrogels in this study.

SEM imaging showed no observable changes in the microstructure of uncrosslinked and crosslinked CMA hydrogels (Figure 3). This finding is consistent with Gaudet and Shreiber's work on photochemically crosslinked CMA using I-2959 photoinitiator [31].

However, recent work has shown that photochemical crosslinking of highly concentrated CMA (i.e., 8 mg/ml) may induce merging of the collagen fibrils in the microstructure, leading to a reduction in pore size [18]. In addition, Yan et al., have shown that genipin crosslinking alters the morphology of collagen/chitosan scaffolds with higher chitosan content [35]. On the contrary, Gaudet and Shrieber, as well as the current study, used lower concentration (i.e., 3 mg/mL) of CMA, suggesting that the effect of crosslinking on the microstructure of CMA hydrogels may be heavily dependent upon the concentration of CMA [17,18,31]. Lower concentration of CMA used in the current study may have allowed for greater porosity between collagen fibrils, allowing them to remain individualized through the crosslinking process.

Mechanical testing entailed evaluating the effect of different crosslinking conditions on the compressive modulus of the CMA hydrogels by determining the slope of the elastic region of the stress-strain curve (Figure 4) [28,36]. The compressive modulus of the CMA hydrogels was observed to significantly increase ($p < 0.05$) after photochemical crosslinking, with further increase upon the addition of genipin crosslinking (Figure 4B). Sung *et al.* observed similar results with a dual crosslinking approach involving genipin, carbodiimide, and EDC [37]. The collagenase degradation study was utilized to replicate the *in vivo* enzymatic environment and further reinforce the benefit of the dual crosslinking strategy [37]. Both photochemical and genipin crosslinked CMA were shown to significantly decrease ($p < 0.05$) the degradation rate of the hydrogels, with dual crosslinking further decreasing ($p < 0.05$) this rate suggesting that dual crosslinking improves the stability of the CMA hydrogels (Figure 5). This improvement in the properties of CMA hydrogels upon dual crosslinking can be attributed to higher crosslinking degree attained via photo-initiated crosslinking of methacrylate groups and genipin mediated crosslinking of the free-amine groups within the collagen structure. In addition, the substantial improvement in the properties of acellular hydrogels (Figure 9) compared to cell-laden hydrogels (Figures 4 and 5) further corroborates that degree of crosslinking of CMA hydrogels can be controlled by modulating the crosslinking conditions of the second step of the dual crosslinking scheme (i.e., genipin crosslinking) [30,38]. These results are consistent with previous studies that explored the impact of dual crosslinking strategies on the stability of collagen-based hydrogels [12,37].

The live-dead assessment of low and high genipin crosslinking with cells embedded in the hydrogel, and by extension low and high dual crosslinking, displayed a significant reduction ($p < 0.05$) in viability for high genipin crosslinking over that of low genipin (Figure 6). Results from the AlamarBlue cell metabolic assay displayed a similar trend (Figure 7), showing a significant decrease ($p < 0.05$) in the metabolic activity on high genipin crosslinked cell-laden CMA hydrogels. These results are consistent with the findings reported by Macaya *et al.* who showed that exposure to 1 mM genipin resulted in a significant decrease in cell viability (i.e., < 60%) [15]. On the other hand, Kim *et al.* showed that cell viability in encapsulated hydrogels remains greater than 90% even at 3 mM genipin concentrations after 1 hour [23]. This discrepancy in cell viability outcomes may be because the extent of genipin cytotoxicity can vary depending on cell type. While Macaya *et al.* and the current study employed hMSC, the study by Kim *et al.* used human adipose stem cells. Based on the cell viability results in the current study, employing low concentrations of

genipin (i.e., <1 mM) is recommended to retain cellular viability within cell-laden constructs. Cell encapsulation allows for greater biomimicry of the natural ECM through three-dimensional scaffolding, and the potential to move towards 3D bioprinting [21–23].

Perhaps the technology that receives the most benefit from the development of an effective dual crosslinking strategy is that of 3D bioprinting. This technology, through application of extruder heads or lithographic techniques, allows for construction of biomimetic scaffolding from natural polymers such as collagen type-I [3,6]. However, the layer by layer nature of many bioprinting techniques limit the type of bioinks that can be used to those that are, or conjugated to, structurally stable polymers [2,39,40]. This can be clearly seen in Figure 7B, wherein a soft material such as pure 3 mg/mL collagen disintegrates without structural stability to survive melting of the FRESH medium. The addition of photochemical crosslinking allows for these constructs to survive the printing process (Figure 8C), which may then be further stabilized with genipin crosslinking (Figure 8D and 8E), with no significant loss of fidelity (Figure 7F–H). A low dual crosslinking methodology was also proven to minimally affect cellular viability on these hMSC laden constructs (Figure 8I and 8J).

Although cell-laden scaffolds have the potential to promote accelerated tissue regeneration due to the presence of pre-seeded regenerative cell population, acellular scaffolds that rely on host cells post implantation are often preferred due to ease of implantation (i.e., no priming of scaffold with cells prior to implantation) and relatively less complex regulatory requirements [41,42]. While a plethora of different acellular scaffolds have been developed, both natural and synthetic, pure collagen-based scaffolds are of singular importance because of their biocompatibility, biodegradability, and the presence of bioactive cell-binding sequences (i.e., RGD). In addition, the use of pure collagen-based bioinks enables bioprinting of a biomimetic scaffold that resembles the physicochemical properties of native tissue. As evidenced in the current study, the generation of cell-laden collagen scaffolds mandates careful use of crosslinking agents in order to maintain a delicate balance between cell viability and scaffold mechanical properties; however, an acellular approach allows for the use of far greater concentrations of genipin, and thus yield scaffolds with significantly greater mechanical and degradation properties. Results from the acellular work demonstrate that dual crosslinking resulted in a significant increase (i.e., up to 5-fold) in the total degradation time (Figure 9B) and compressive modulus (Figure 9C) of 3D CMA hydrogels. While the use of genipin only can yield similar outcomes, dual crosslinking is essential for bioprinting purposes since the 3D printed constructs do not survive the FRESH melting process if not photochemically crosslinked (Figure 8B and 8D). The dual crosslinking strategy developed in this study can be leveraged in different additive manufacturing practices for 3D bioprinting of mechanically robust and stable collagen-based acellular scaffolds with pre-defined complex geometries and controlled pore structure for use in a variety of different tissue engineering applications.

The use of pure collagen-based solutions as bioinks reduces bioink material requirements for structural stability and thus opens up a plethora of different prospects for the development of biomimetic scaffolds for tissue engineering applications [2,43]. Results from this study demonstrate that sequential application of photochemical crosslinking and genipin

crosslinking have the potential to overcome limitations associated with weak mechanical properties and fast degradation that are inherent to constructs fabricated using low concentrations of collagen. While application of dual crosslinking resulted in substantial improvement in the mechanical and degradation properties of acellular CMA hydrogels, it is important to note that this strategy may not be immediately applicable for tissue engineering purposes with cell-laden hydrogels due to a relatively small improvement in CMA hydrogel properties. Nevertheless, results from the current study provide a solid and statistically significant foundation to warrant further investigation on the development of alternative strategies to improve the mechanical and degradation properties of cell-laden CMA hydrogels for their clinical use. These strategies can include identifying alternative biocompatible crosslinking regimens or *in vitro* culturing of cell-laden hydrogels to enable cell-mediated remodeling of the hydrogel prior to implantation. Overall, dual crosslinking strategy developed in this study is a promising approach for 3D bioprinting of mechanically viable cell-laden collagen-based constructs.

Acknowledgments:

This study was supported by a grant from National Institute of Health (NIH 1R15AR071102). The content reported here is solely the responsibility of the authors and does not necessarily represent the official views of the NIH.

References:

[1]. Thomas DJ, 3-D bioprinting transplantable tissue structures: A perspective for future reconstructive surgical transplantation, Bioprinting. 1–2 (2016) 36–37. doi:10.1016/j.bprint.2016.08.002.

[2]. Aljohani W, Ullah MW, Zhang X, Yang G, Bioprinting and its applications in tissue engineering and regenerative medicine, Int. J. Biol. Macromol 107 (2018) 261–275. doi:10.1016/j.ijbiomac.2017.08.171. [PubMed: 28870749]

[3]. Mandrycky C, Wang Z, Kim K, Kim DH, 3D bioprinting for engineering complex tissues, Biotechnol. Adv 34 (2016) 422–434. doi:10.1016/j.biotechadv.2015.12.011. [PubMed: 26724184]

[4]. Webb B, Doyle BJ, Parameter optimization for 3D bioprinting of hydrogels, Bioprinting. 8 (2017) 8–12. doi:10.1016/j.bprint.2017.09.001.

[5]. Chimene D, Lennox KK, Kaunas RR, Gaharwar AK, Advanced Bioinks for 3D Printing: A Materials Science Perspective, Ann. Biomed. Eng 44 (2016) 2090–2102. doi: 10.1007/s10439-016-1638-y. [PubMed: 27184494]

[6]. Hospodiuk M, Dey M, Sosnoski D, Ozbolat IT, The bioink: A comprehensive review on bioprintable materials, Biotechnol. Adv 35 (2017) 217–239. doi: 10.1016/j.biotechadv.2016.12.006. [PubMed: 28057483]

[7]. Chung JHY, Naficy S, Yue Z, Kapsa R, Quigley A, Moulton SE, Wallace GG, Bioink properties and printability for extrusion printing living cells, Biomater. Sci 1 (2013) 763–773. doi:10.1039/c3bm00012e.

[8]. Lee KY, Mooney DJ, Alginate: Properties and biomedical applications, Prog. Polym. Sci 37 (2012) 106–126. doi:10.1016/j.progpolymsci.2011.06.003. [PubMed: 22125349]

[9]. Van Uden S, Silva-correia J, Oliveira JM, Reis RL, Current strategies for treatment of intervertebral disc degeneration : substitution and regeneration possibilities, (2017) 1–19. doi: 10.1186/s40824-017-0106-6.

[10]. Diamantides N, Wang L, Pruiksma T, Siemiatkoski J, Dugopolski C, Correlating rheological properties and printability of collagen bioinks : the effects of riboflavin photocrosslinking and pH Correlating rheological properties and printability of collagen bioinks : the effects of ribo fl avin photocrosslinking and pH, (2017).

[11]. Gopinathan J, Noh I, Recent trends in bioinks for 3D printing, Biomater. Res 22 (2018) 1–15. doi:10.1186/s40824-018-0122-1. [PubMed: 29308274]

[12]. Omobono MA, Zhao X, Furlong MA, Kwon CH, Gill TJ, Randolph MA, Redmond RW, Enhancing the stiffness of collagen hydrogels for delivery of encapsulated chondrocytes to articular lesions for cartilage regeneration, J. Biomed. Mater. Res. - Part A. 103 (2015) 1332–1338. doi:10.1002/jbm.a.35266.

[13]. Rodriguez-Pascual F, Slatter DA, Collagen cross-linking: Insights on the evolution of metazoan extracellular matrix, Sci. Rep 6 (2016) 1–7. doi:10.1038/srep37374. [PubMed: 28442746]

[14]. Nichol JW, Koshy ST, Bae H, Hwang CM, Yamanlar S, Khademhosseini A, Cell-laden microengineered gelatin methacrylate hydrogels, Biomaterials. 31 (2010) 5536–5544. doi: 10.1016/j.biomaterials.2010.03.064. [PubMed: 20417964]

[15]. MacAya D, Ng KK, Spector M, Injectable collagen-genipin gel for the treatment of spinal cord injury: In vitro studies, Adv. Funct. Mater. 21 (2011) 4788–4797. doi: 10.1002/adfm.201101720.

[16]. Madhavan K, Belchenko D, Motta A, Tan W, Evaluation of composition and crosslinking effects on collagen-based composite constructs, Acta Biomater 6 (2010) 1413–1422. doi:10.1016/j.actbio.2009.09.028. [PubMed: 19815100]

[17]. Drzewiecki KE, Parmar AS, Gaudet ID, Branch JR, Pike DH, Nanda V, Shreiber DI, Methacrylation Induces Rapid, Temperature-Dependent, Reversible Self-Assembly of Type □ I Collagen, (2014).

[18]. Nguyen T, Watkins KE, Kishore V, Photochemically Crosslinked Cell □laden Methacrylated Collagen Hydrogels with High Cell Viability and Functionality, J. Biomed. Mater. Res. - Part A. (2019) 1–10. doi:10.1002/jbm.a.36668.

[19]. Fenn SL, Oldinski RA, Visible light crosslinking of methacrylated hyaluronan hydrogels for injectable tissue repair, (2015) 1229–1236. doi:10.1002/jbm.b.33476.

[20]. Rouillard AD, Berglund CM, Lee JY, Polacheck WJ, Tsui Y, Bonassar LJ, Kirby BJ, Methods for Photocrosslinking Alginate Hydrogel Scaffolds with High Cell Viability, Tissue Eng. Part C Methods. 17 (2011) 173–179. doi:10.1089/ten.tec.2009.0582. [PubMed: 20704471]

[21]. Knowlton S, Yenilmez B, Anand S, Tasoglu S, Photocrosslinking-based bioprinting: Examining crosslinking schemes, Bioprinting. 5 (2017) 10–18. doi:10.1016/j.bprint.2017.03.001.

[22]. Ibusuki S, Halbesma GJ, Randolph MA, Redmond RW, Kochevar IE, Gill TJ, Photochemically Cross-Linked Collagen Gels as Three-Dimensional Scaffolds for Tissue Engineering, Tissue Eng 13 (2007) 1995–2001. doi:10.1089/ten.2006.0153. [PubMed: 17518705]

[23]. Kim YB, Lee H, Kim GH, Strategy to Achieve Highly Porous/Biocompatible Macroscale Cell Blocks, Using a Collagen/Genipin-bioink and an Optimal 3D Printing Process, ACS Appl. Mater. Interfaces. 8 (2016) 32230–32240. doi:10.1021/acsami.6b11669. [PubMed: 27933843]

[24]. Macaya D, Ng KK, Spector M, Injectable Collagen - Genipin Gel for the Treatment of Spinal Cord Injury: In Vitro Studies, (2011) 4788–4797. doi:10.1002/adfm.201101720.

[25]. Sundararaghavan HG, Monteiro GA, Lapin NA, Chabal YJ, Miksan JR, Shreiber DI, Genipin-induced changes in collagen gels: Correlation of mechanical properties to fluorescence, J. Biomed. Mater. Res. - Part A. 87 (2008) 308–320. doi:10.1002/jbm.a.31715.

[26]. Sechriest VF, Miao YJ, Niyibizi C, Westerhausen-Larson A, Matthew HW, Evans CH, Fu FH, Suh JK, GAG-augmented polysaccharide hydrogel: A novel biocompatible and biodegradable material to support chondrogenesis, J. Biomed. Mater. Res 49 (2000) 534–541. doi:10.1002/(SICI)1097-4636(20000315)49:4<534::AID-JBM12>3.0.C0;2-#. [PubMed: 10602087]

[27]. Helary C, Bataille I, Abed A, Illoul C, Anglo A, Louedec L, Letourneur D, Meddahi-Pelle A, Giraud-Guille MM, Concentrated collagen hydrogels as dermal substitutes, Biomaterials. 31 (2010) 481–490. doi:10.1016/j.biomaterials.2009.09.073. [PubMed: 19811818]

[28]. Worthington KS, Wiley LA, Bartlett AM, Stone EM, Mullins RF, Salem AK, Guymon CA, Tucker BA, Mechanical properties of murine and porcine ocular tissues in compression, Exp. Eye Res 121 (2014) 194–199. doi:10.1016/j.exer.2014.02.020. [PubMed: 24613781]

[29]. Hinton TJ, Jallerat Q, Palchesko RN, Park JH, Grodzicki MS, Shue HJ, Ramadan MH, Hudson AR, Feinberg AW, Three-dimensional printing of complex biological structures by freeform reversible embedding of suspended hydrogels, Sci. Adv 1 (2015). doi:10.1126/sciadv.1500758.

[30]. Alfredo J, Kishore V, Akkus O, Alfredo Uquillas J, Kishore V, Akkus O, Genipin crosslinking elevates the strength of electrochemically aligned collagen to the level of tendons, J. Mech. Behav. Biomed. Mater. 15 (2012) 176–189. doi:10.1016/j.jmbbm.2012.06.012. [PubMed: 23032437]

[31]. Gaudet ID, Shreiber DI, Characterization of methacrylated Type-I collagen as a dynamic, photoactive hydrogel, Biointerphases. 7 (2012) 1–9. doi:10.1007/s13758-012-0025-y. [PubMed: 22589044]

[32]. Fujikawa S, Nakamura S, Koga K, Genipin, a New Type of Protein Crosslinking Reagent from Gardenia Fruits, Agric. Biol. Chem 52 (1988) 869–870. doi:10.1271/bbb1961.52.869.

[33]. Kishore V, Iyer R, Frandsen A, Nguyen TU, In vitro characterization of electrochemically compacted collagen matrices for corneal applications, Biomed. Mater. 11 (2016). doi: 10.1088/1748-6041/11/5/055008.

[34]. Sisson K, Zhang C, Farach-Carson MC, Chase DB, Rabolt JF, Evaluation of cross-linking methods for electrospun gelatin on cell growth and viability, Biomacromolecules. 10 (2009) 1675–1680. doi:10.1021/bm900036s. [PubMed: 19456101]

[35]. Yan L-P, Wang Y-J, Ren L, Wu G, Caridade SG, Fan J-B, Wang L-Y, Ji P-H, Oliveira JM, Oliveira JT, Mano JF, Reis RL, Genipin-cross-linked collagen/chitosan biomimetic scaffolds for articular cartilage tissue engineering applications, J. Biomed. Mater. Res. Part A. 95A (2010) 465–475. doi:doi:10.1002/jbm.a.32869.

[36]. Dhert WJA, Visser J, Mouser VHM, Malda J, Gawlitta D, Melchels FPW, Yield stress determines bioprintability of hydrogels based on gelatin-methacryloyl and gellan gum for cartilage bioprinting, Biofabrication. 8 (2016) 035003. doi:10.1088/1758-5090/8/3/035003.

[37]. Sung H-W, Chang W-H, Ma C-Y, Lee M-H, Crosslinking of biological tissues using genipin, J Biomed Mater Res A. 64 (2003) 427–438. [PubMed: 12579556]

[38]. Bi L, Cao Z, Hu Y, Song Y, Yu L, Yang B, Mu J, Huang Z, Han Y, Effects of different cross-linking conditions on the properties of genipin-cross-linked chitosan/collagen scaffolds for cartilage tissue engineering, J. Mater. Sci. Mater. Med 22 (2011) 51–62. doi:10.1007/s10856-010-4177-3. [PubMed: 21052794]

[39]. Gibson I, Rosen D, Stucker B, Additive Manufacturing Technologies, 2nd ed., Springer, New York, NY, 2015. doi:10.2495/SDP-V9-N5-658-668.

[40]. Ozbolat IT, Moncal KK, Gudapati H, Evaluation of bioprinter technologies, Addit. Manuf 13 (2017) 179–200. doi:10.1016/j.addma.2016.10.003.

[41]. Webber MJ, Khan OF, Sydlik SA, Tang BC, Langer R, A Perspective on the Clinical Translation of Scaffolds for Tissue Engineering, Ann. Biomed. Eng 43 (2015) 641–656. doi:10.1007/s10439-014-1104-7. [PubMed: 25201605]

[42]. O'Brien FJ, Biomaterials & scaffolds for tissue engineering, Mater. Today. 14 (2011) 88–95. doi: 10.1016/S1369-7021(11)70058-X.

[43]. Williams D, Thayer P, Martinez H, Gatenholm E, Khademhosseini A, A perspective on the physical, mechanical and biological specifications of bioinks and the development of functional tissues in 3D bioprinting, Bioprinting. 9 (2018) 19–36.doi: 10.1016/j.bprint.2018.02.003.

Highlights:

- Direct cell exposure to genipin at concentrations greater than 1 mM is cytotoxic
- Dual crosslinking enhances mechanical and degradation properties of CMA hydrogels
- Dual crosslinking maintains viability and print fidelity of cell-laden CMA constructs

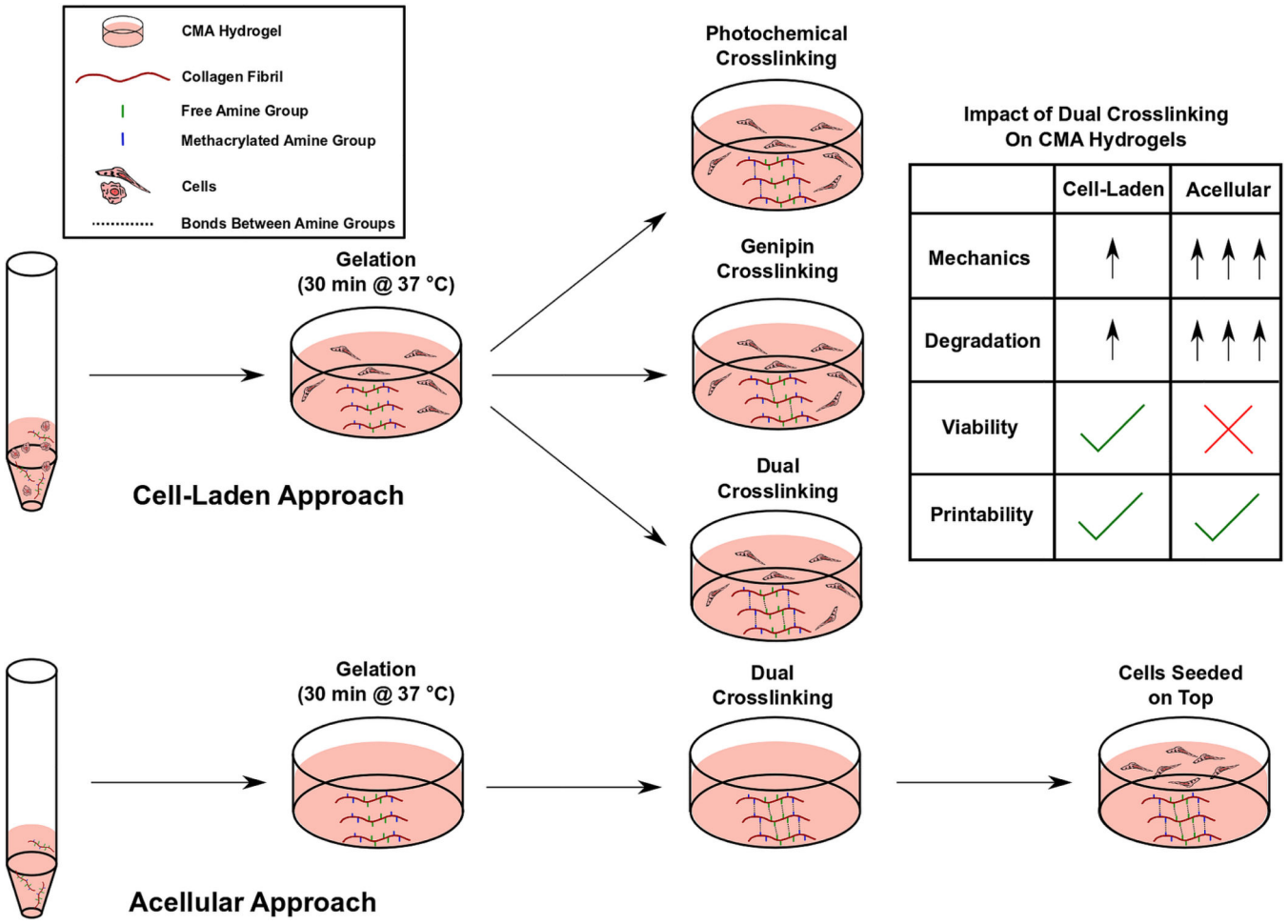

Figure 1.

Schematic illustration of the dual crosslinking strategy for cell-laden and acellular 3D CMA hydrogels.

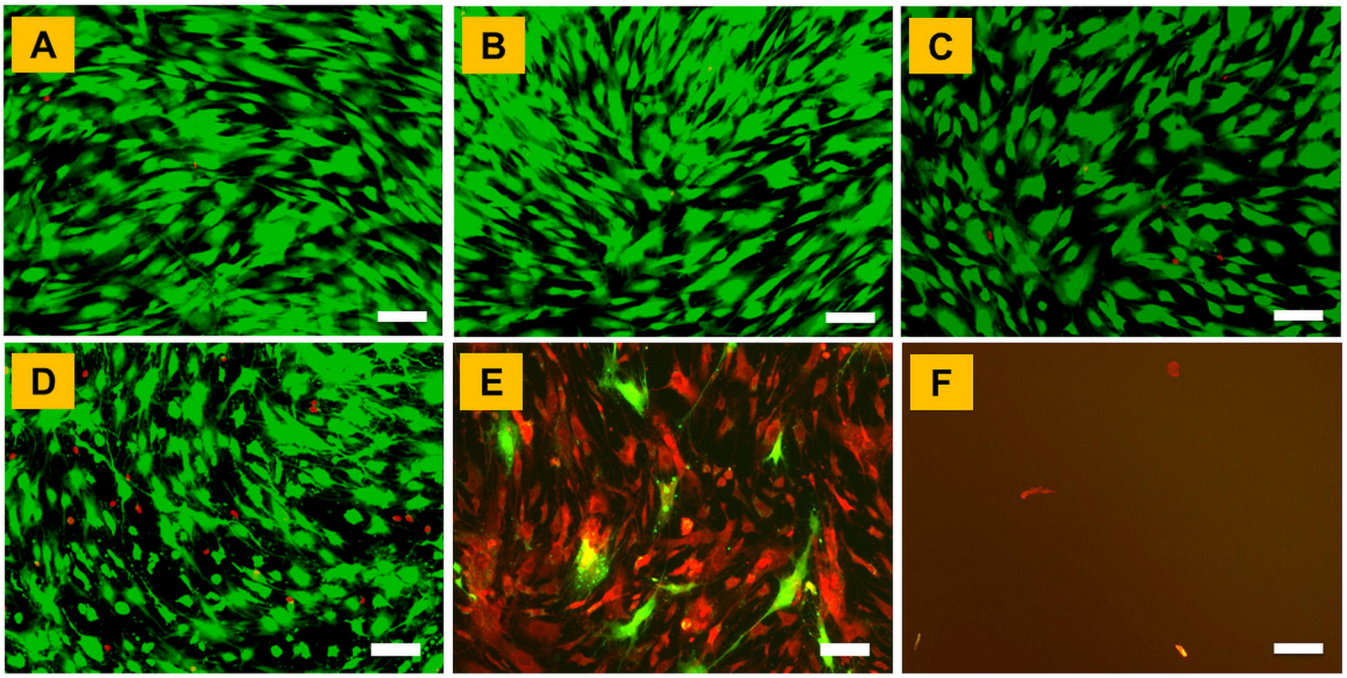

Figure 2.

Cell viability in different concentrations of genipin solution assessed via live-dead assay: (A) 0 mM, (B) 0.25 mM, (C) 0.5 mM, (D) 1 mM, (E) 5 mM, and (F) 10 mM. Scale bar: 100μm.

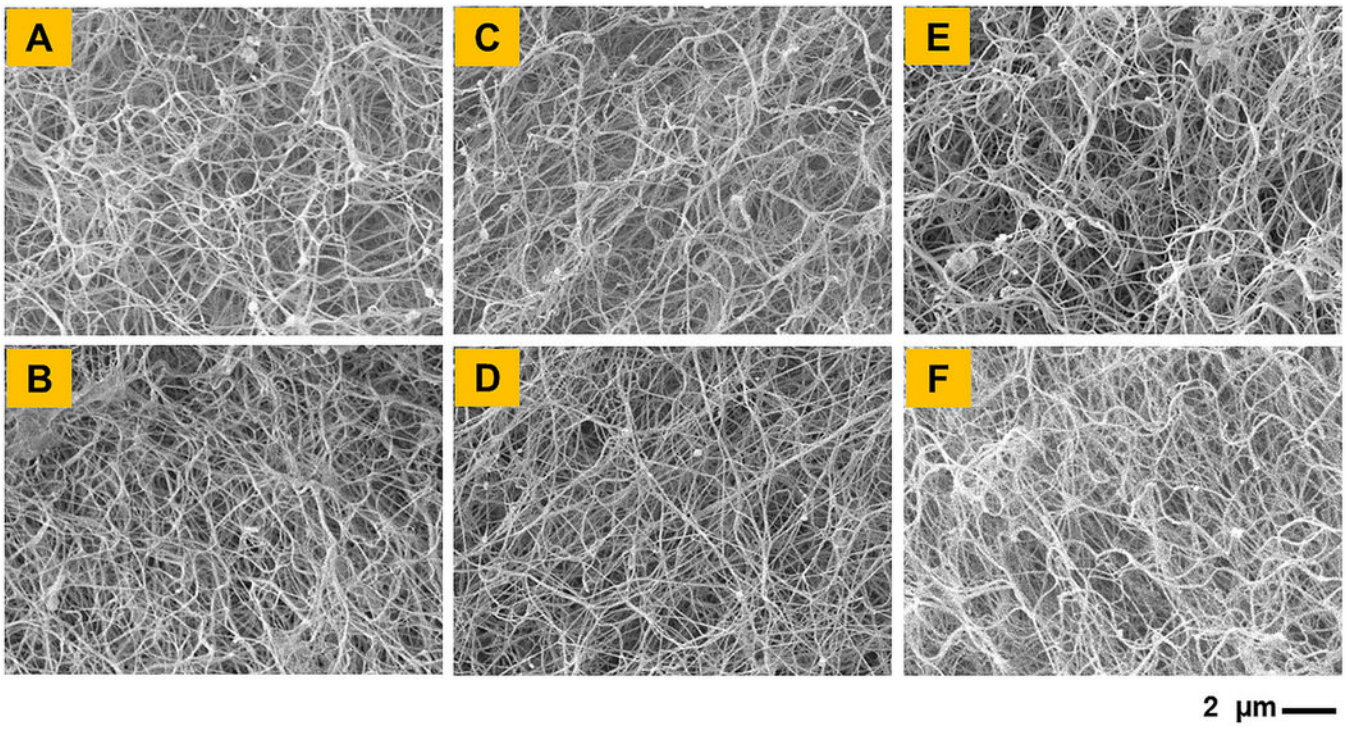

Figure 3.

SEM images show morphology of (A) Uncrosslinked CMA hydrogel and CMA hydrogels crosslinked with (B) 1% VA-086, (C) low genipin, (D) high genipin, (E) low dual, and (F) high dual crosslinking. Scale bar: 2 µm.

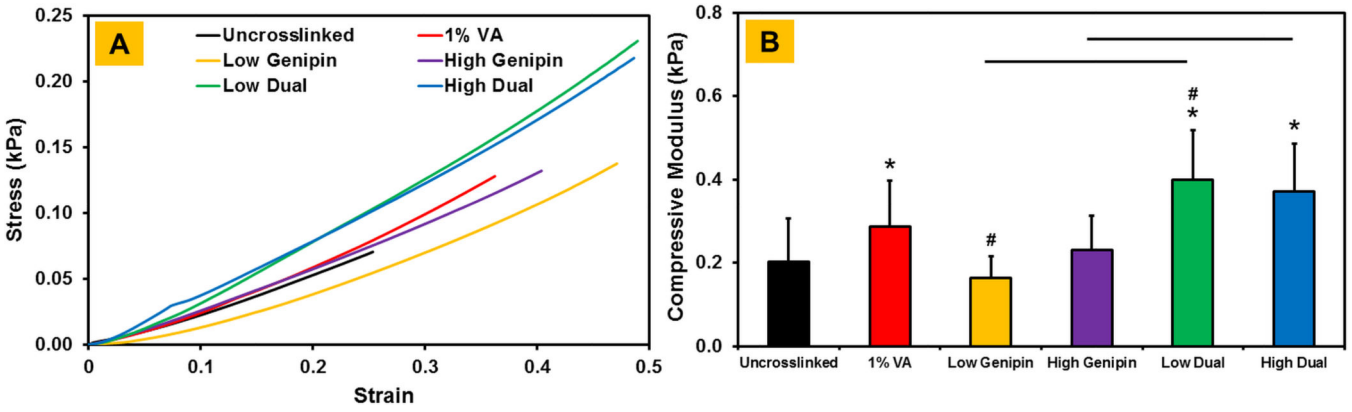

Figure 4.

(A) Representative stress versus strain curves of CMA hydrogels. (B) Compressive modulus of CMA hydrogels (* denotes $p < 0.05$ when comparing crosslinked CMA with uncrosslinked CMA, # denotes $p < 0.05$ when comparing between other crosslinked CMA groups with 1% VA-086 crosslinked CMA, horizontal lines denote $p < 0.05$ between connecting groups).

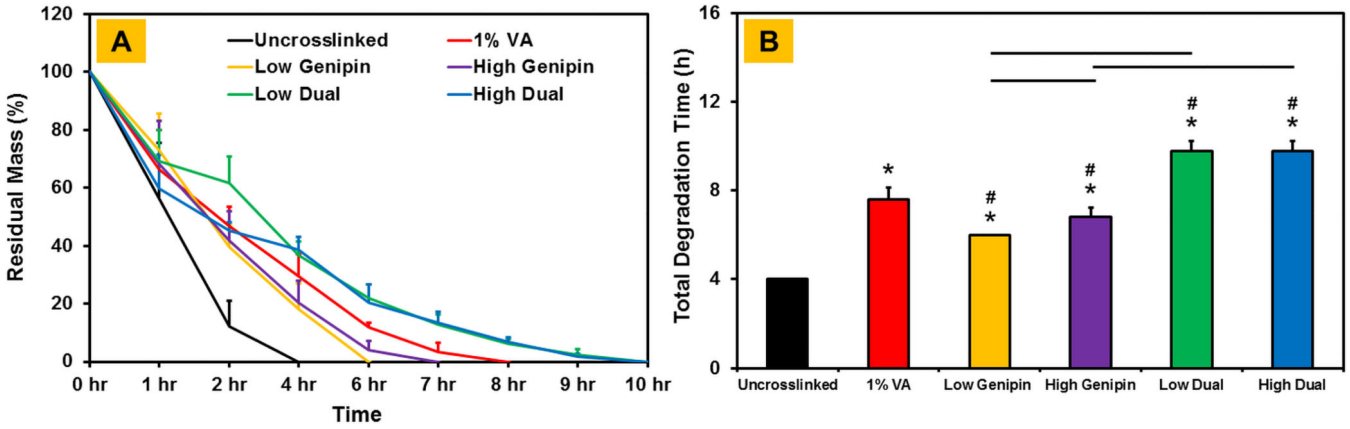

Figure 5.

Assessment of stability of crosslinked CMA hydrogels using *in vitro* collagenase degradation assay (* denotes $p < 0.05$ when comparing crosslinked CMA with uncrosslinked CMA, # denotes $p < 0.05$ when comparing between other crosslinked CMA with 1% VA-086 crosslinked CMA, horizontal lines denote $p < 0.05$ between connecting groups).

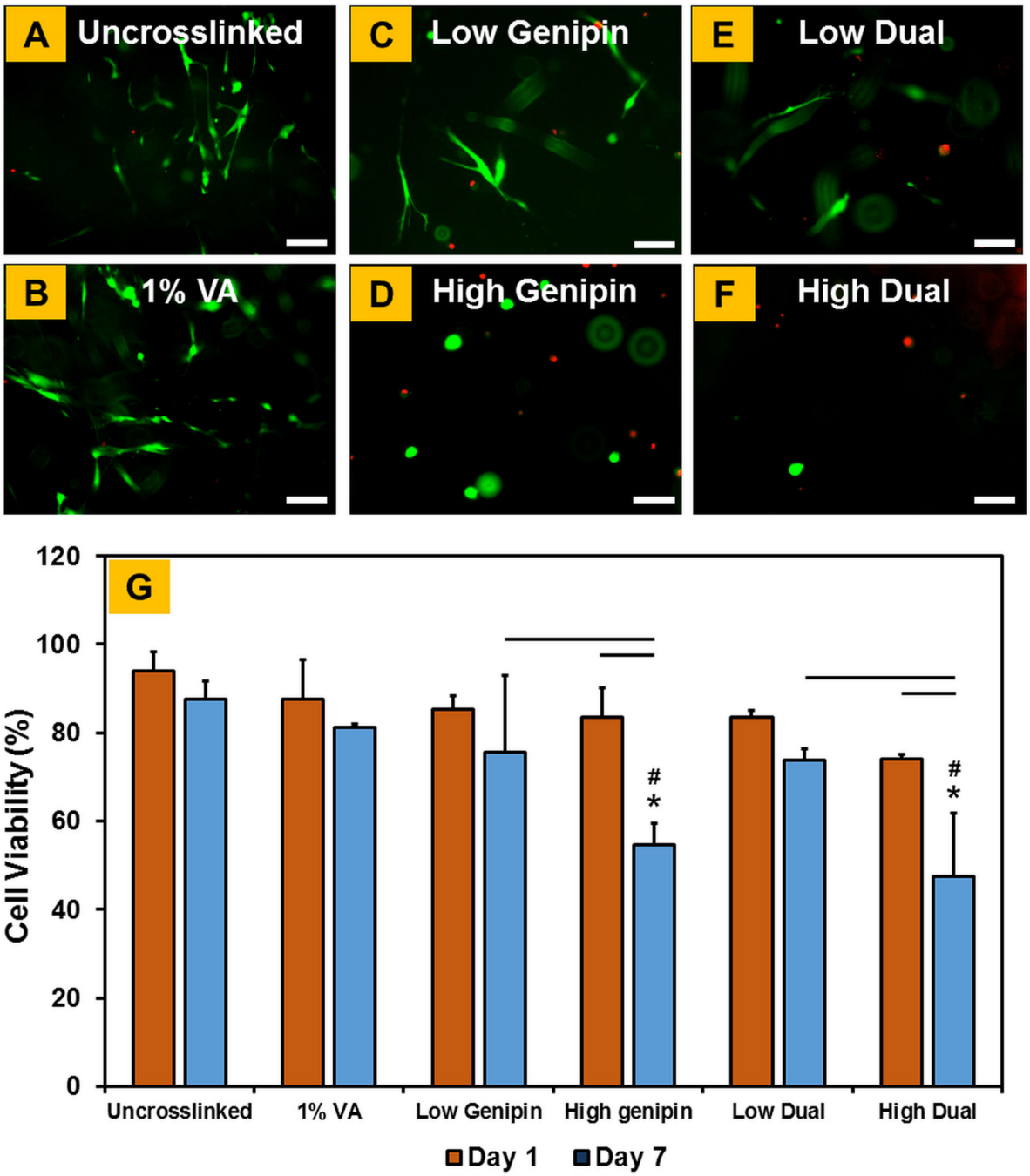

Figure 6.

(A-F) Live-dead assay to assess the viability of hMSCs encapsulated within crosslinked CMA hydrogels (live cells stain green and dead cells stain red). (G) Quantification of cell viability plot (* denotes $p < 0.05$ when comparing crosslinked CMA with uncrosslinked CMA, # denotes $p < 0.05$ when comparing between other crosslinked CMA with 1% VA-086 crosslinked CMA, horizontal lines denote $p < 0.05$ between connecting groups). Scale bar: 100μm

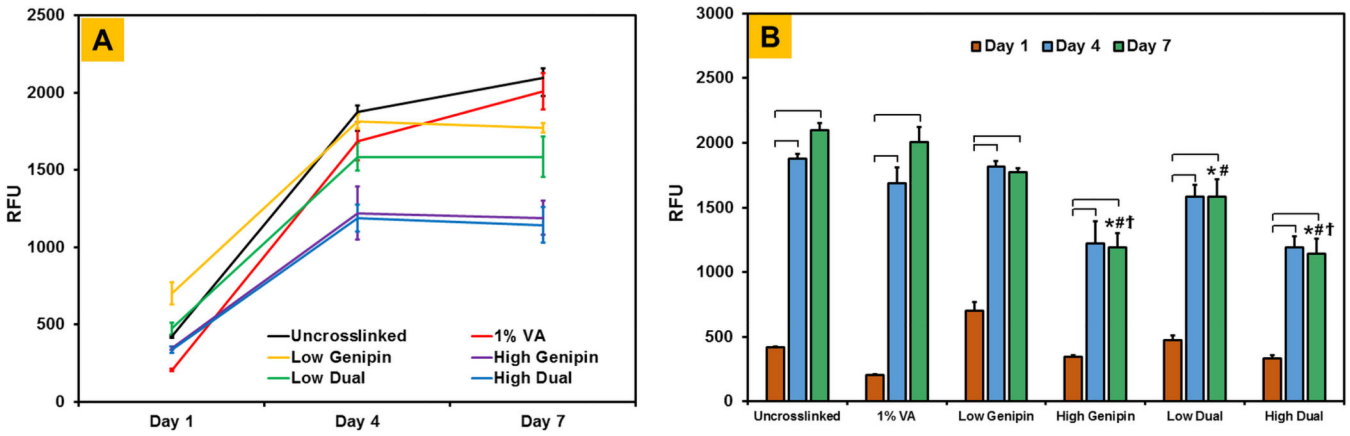

Figure 7.

Quantification of cell metabolic activity on crosslinked CMA hydrogels using AlamarBlue assay (* denotes $p < 0.05$ when comparing crosslinked CMA with uncrosslinked CMA at corresponding time point, # denotes $p < 0.05$ when comparing between other crosslinked CMA with 1% VA-086 crosslinked CMA at corresponding time point, † denotes $p < 0.05$ when comparing between CMA hydrogels crosslinked with low concentration of genipin versus high concentration of genipin at corresponding time point, brackets denote $p < 0.05$ between connecting groups).

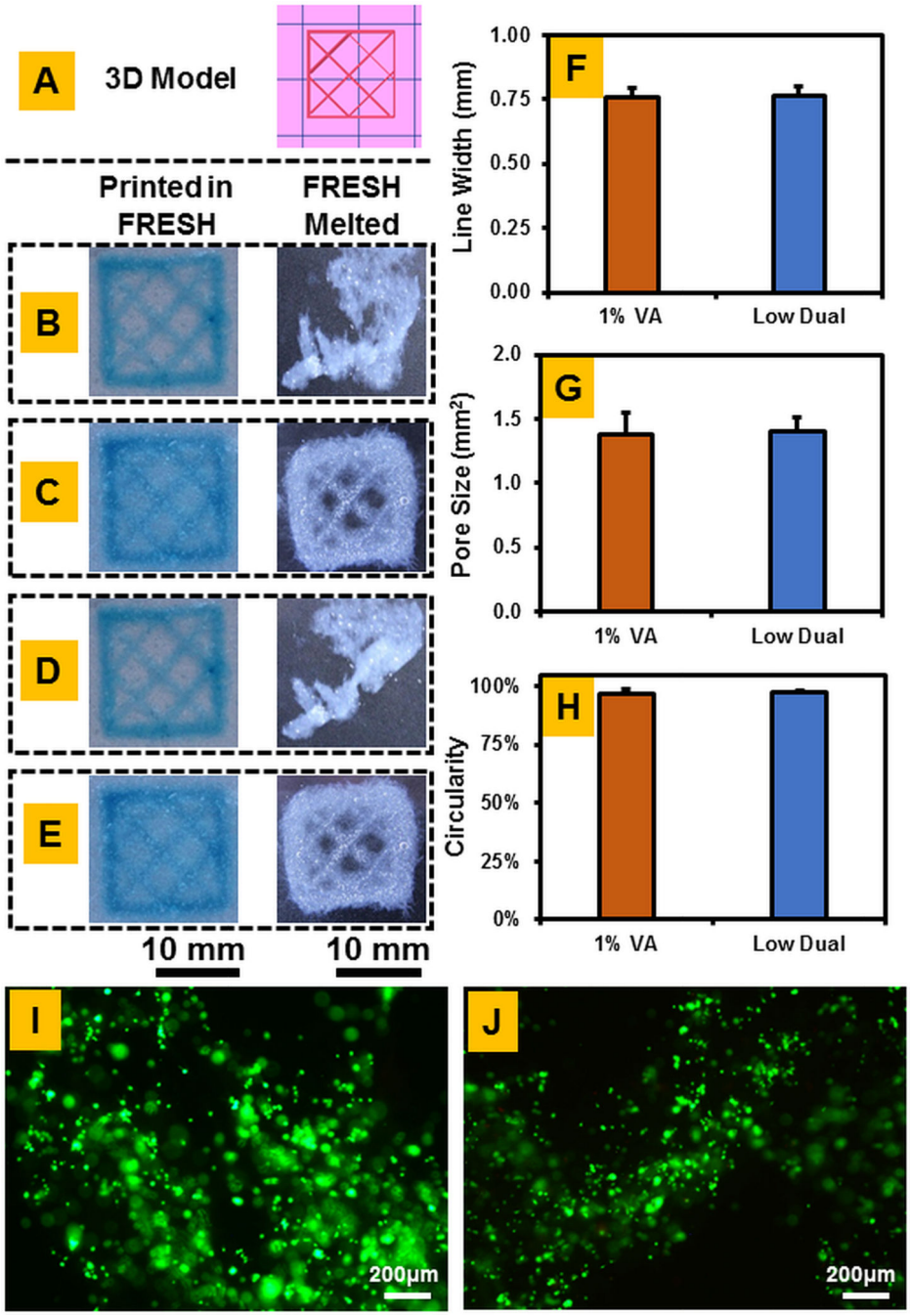

Figure 8.

3D Bioprinted CMA Construct evaluation: (A) Original 3D Model, (B) Uncrosslinked construct, (C) 1% VA Photoinitiated crosslinked construct, (D) Low genipin only crosslinked construct, (E) Dual crosslinked construct, (F) Line width determination of inner mesh, (G) Pore size evaluation of inner mesh, (H) Circularity for circular construct, (I) Cell viability for 1% VA photochemically crosslinked construct, (J) Cell viability for dual crosslinked construct. Print fidelity measurements for uncrosslinked and low genipin

crosslinked constructs were not feasible because the constructs deformed after melting of the FRESH media.

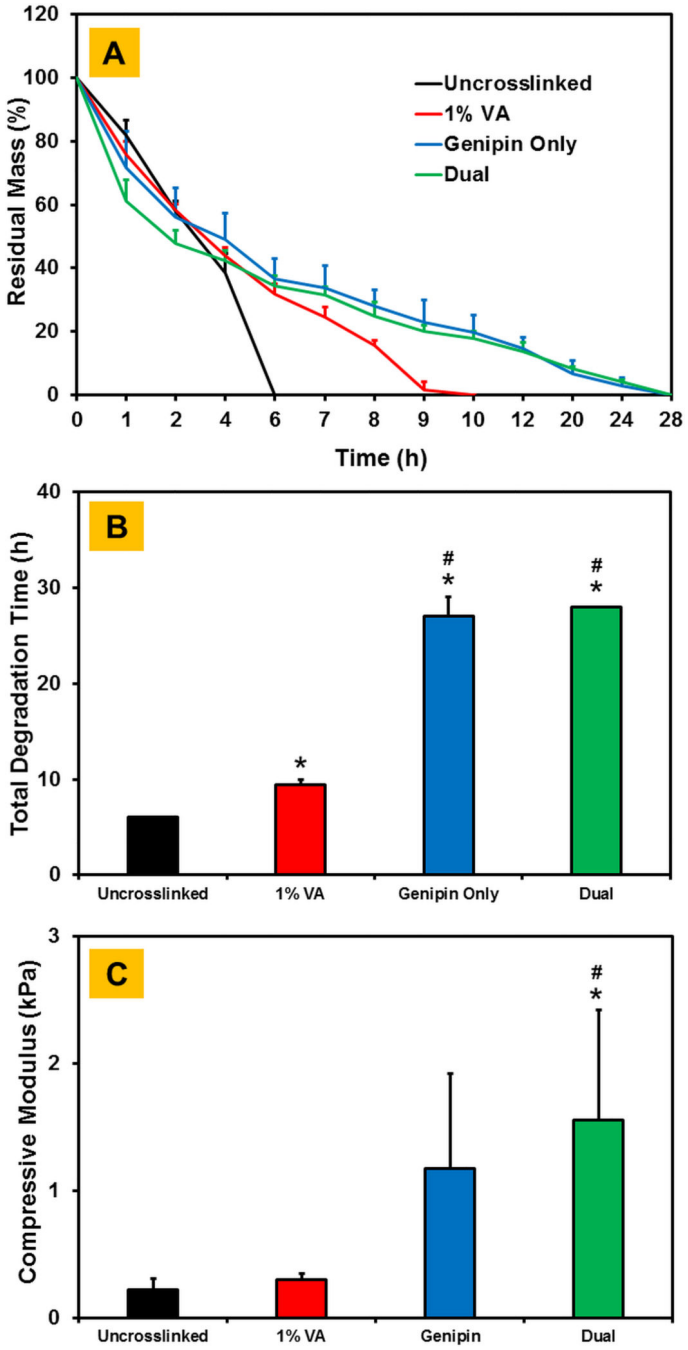

Figure 9.

Assessment of stability and compressive modulus of crosslinked CMA hydrogels in a cell free approach (A) Line plot showing change in residual mass with time, (B) Comparison of total degradation time between different crosslinked CMA hydrogels, (C) Compressive modulus of uncrosslinked, single and dual crosslinked CMA hydrogels with 1% VA-086 and 28 mM genipin in 90% ethanol for 24 h (* denotes $p < 0.05$ when comparing crosslinked

CMA with uncrosslinked CMA, # denotes $p < 0.05$ when comparing between other crosslinked CMA with 1% VA-086 crosslinked CMA).

Table 1:

Parameters for Bioprinting of Cell-laden Constructs

Parameter	Value	Description
Tip Diameter	0.21mm	A blunt syringe tip for the print head
Tip Gauge	27g	
Print Shape	Cube	Outer limit of construct is square
Infill Pattern	Mesh	Inner pattern is cross-hatched
Infill Angle	45°	The angle at which the bioink was extruded
Flow Speed	5 mm/s	Extrusion speed for optimal density
Crosslink Power	11mW/cm^2	Power density of UV crosslinking
Crosslink Time	60s	Time exposure of UV for crosslinking